Nonlinear spectral blue shift in semicondutor optical amplifiers

A. E. Bednyakova[1,2,*], D. Khudozhitkova[1], A. Kokhanovskiy[1], and S. K. Turitsyn[1,3]

[1] Novosibirsk State University, Novosibirsk 630090, Russia
[2] Institute of Computational Technologies, SB RAS, Novosibirsk 630090, Russia
[3] Aston Institute of Photonic Technologies, Aston University, Birmingham B4 7ET, UK
[*] anastasia.bednyakova@gmail.com

Compiled August 24, 2021

We demonstrate that spectral peak power of negatively chirped optical pulses can acquire a blue-shift after amplification by the semiconductor optical amplifier. The central wavelength of a transform limited optical pulse translates over 20 nm towards a shorter wavelength after propagation in the single-mode fiber and semiconductor optical amplifier. A chirped Guassian pulse with the full width at half maximum 1 ps and the dimensionless chirp parameter C=-20 can be blue-shifted by 5 THz.

http://dx.doi.org/10.1364/ao.XX.XXXXXX

In the seminal paper [1] Mitschke and Mollenauer discovered a continuous shift in the optical frequency of a soliton pulse propagating down the optical fiber. This is a manifestation of the nonlinear phenomenon caused by a Raman-induced energy spectral transfer from the lower to higher wavelengths (redshift). Gordon in [2] has introduced a theory of the Raman self-frequency shift for a pulse propagating in optical fibers. A possibility to shift central frequency of the optical pulse (soliton) to the red part of the spectrum in a controllable manner paved the way for a variety of practical applications including frequency converters and spectrally tunable optical pulsed sources. The key attractive feature of the Raman soliton self-frequency shift for applications is a possibility of a wavelength conversion to the spectral intervals that are not covered by easily available light sources. Due to the generic nature of the Raman effect a spectral redshift is nowadays a well established practical technique. However, there is no comparable easily-implementable general method to produce blueshift of the spectral peak of radiation.

Note that the stimulated Stokes Raman scattering is always accompanied by the anti-Stokes Raman scattering that produces wave at shorter wavelength (or higher frequences). However, efficiency of the coherent anti-Stokes scattering is typically much lower compared to the non-spontaneous Raman process that is a dominant effect in a variety of conventional materials. Anti-Stokes Raman scattering can be enhanced in waveguides [3] and through special designs of such wavelength converters (for advances in this field, see e.g. recent review [4] and references therein).

Blue shift of the radiation can be achieved by using higher-order harmonics generation. Second and third harmonics are routingly used for light up-conversion. High-order harmonics [5, 6] (more than 25 harmonics) can be used for generation of extreme ultra-violet radiation. Parametric processes supported by the Kerr nonlinearity, more specifically, four-wave-mixing and cross-phase modulation are successfully used for light up-conversion [7–10]. In [11–13] effect of the spectral blueshift was studied and experimentally demonstrated. It has been shown in [12, 13] that the photoionization effect (when the intensity of solitons is slightly above the photoionization threshold) in a hollow-core photonic crystal fiber filled with a Raman-inactive noble gas produced a constant acceleration of solitons in the time domain with a continuous shift to higher frequencies. Among the key challenges of the existing up-conversion techniques is efficiency of such processes. In this Letter we propose relatively simple alternative possibility to achieve blueshift of optical pulses using commercially available semiconductor optical amplifier.

The semiconductor optical amplifier (SOA) is an important practical device developed for optical communication systems. The SOA exhibits many attractive characteristics, including compactness, low power consumption, and wide gain bandwidth. Beyond direct applications as an amplifier SOA is used in all-optical signal processing, and applications such as radio over fiber, modulators and emerging neuromorphic photonics [7, 14–16]. SOA transformed the field of nonlinear optical techniques for data processing at high speed. SOA can operate at 100 gigabits per second and higher [14]. SOA is also an example of the physical system with interesting nonlinear properties, often considered by engineers as a drawback and undesirable feature of the device.

The transmission characteristics of the SOA are described by a conventional rate equation for the carrier density and a linear relationship between the carrier density and the induced complex susceptibility [17]. Neglecting the dispersion within the SOA, the transient response is modelled [17] by a time-dependent gain $h(t)$ and a linewidth enhancement factor α_H as:

$$\begin{aligned} A_{out}(t) &= \exp\left[(1-i\alpha_H)h(t)/2\right] A_{in}(t), \\ \frac{dh}{dt} &= -\frac{h-h_0}{T_{SOA}} - \frac{|A_{in}(t)|^2}{E_{sat}}\left[\exp(h)-1\right], \end{aligned} \tag{1}$$

where $A_{in}(t)$ and $A_{out}(t)$ are, respectively the input and output optical fields, h_0 is related to the small signal gain $G_0 = \exp(h_0)$,

T_{SOA} the gain recovery time, E_{sat} is a characteristic saturation energy that defines the SOA saturation power $P_{sat} = E_{sat}/T_{SOA}$, and α_H is the so-called Henry linewidth enhancement factor. We consider without loss of generality the following typical parameters: $\alpha_H = 5$, $E_{sat} = 8$ pJ, $T_{SOA} = 200$ ps for all numerical modeling hereinafter.

We examine here application of the SOA as a nonlinear device that transforms the input signal $A_{in}(t)$ into the field $A_{out}(t) = \sqrt{P_{out}} \times \exp[i\phi_{out}]$. The Eq. 1 cannot be solved analytically, therefore, we examine numerically the transformation of the initially chirped Gaussian pulse having the form $A_{in}(t) = \sqrt{P_0}\exp[-\frac{1+iC}{2}\frac{t^2}{\tau^2}]$.

In the limit $\tau \ll T_{SOA}$, we can use a well-known approximated solution of Eq. (1) [17]:

$$h(t) = -\ln[1 - (1 - \frac{1}{G_0})\exp(-\frac{U_{in}(t)}{E_{sat}})]$$

where $U_{in}(t) = \int_{-\infty}^{t} P_{in}(s)ds$. In this limit the output pulse power and the instantaneous frequency $\Omega_{out} = d\phi_{out}/dt$ are: [17]:

$$P_{out}(t) = P_{in}(t)\exp[h(t)] = \frac{E_{sat}\,G_0}{G_0 - 1} \times \frac{dh}{dt}, \tag{2}$$

$$\frac{d\phi_{out}}{dt} + C\frac{t}{\tau^2} = \frac{\alpha_H}{2}\frac{dh}{dt} = -\frac{\alpha_H(G_0-1)}{2G_0E_{sat}} \times P_{out}(t) \tag{3}$$

Input signal (chirped Gaussian pulse) is nonlinearly transformed by SOA. This functional transformation depends on the input signal parameters (τ, P_{in}, C) and SOA parameters (gain G_0 and the Henry factor α_H). This makes challenging full characterisation of the SOA-based nonlinear transformation. Though the output pulse is not having Gaussian shape after SOA-transformation, we can highlight several important features of the input-output mapping. Our focus will be on the output pulse spectrum. More specifically, we examine a possibility of the control of the spectral shift of the peak of pulse spectrum by varying input field characteristics.

The nonlinear transformation implemented with SOA is illustrated by Figs. 1-3.

Figure 1 shows shift of the central wavelength (peak of the spectral power distribution) of initially chirped Gaussian pulse with 1 ps duration and varying peak power. For positive and small negative chirp $C > -5$ pulse spectrum shifts to red side, having a stationary point in the vicinity of $C = -5$ (white line in Fig. 1a). This is a well-known and studied effect [17]. If the absolute value of chirp increases $C < -5$, blue shift takes place.

Transformation of temporal shape, spectrum and instant frequency, corresponding to negative chirp $C = -20$, is shown in Fig. 2. Peak power growth leads to increase of the spectrum shift to the blue side due to influence of SPM-induced term in eq. (3). Temporal pulse shift is also getting larger. Fig. 2c shows SPM-induced frequency chirp imposed on the pulse as it propagates through the amplifier.

Visualization of nonlinear pulse transformation in spectral and temporal domain simultaneously can be done with a spectrogram. Figure 3 depicts spectograms, corresponding to several values of the input chirp. Arrows point out direction of the pulse peak shift in the time-frequency space. Note, that pulse shape $P_{out}(t)$ and its temporal shift do not depend on initial chirp (see eq.(2)), so the x-coordinate of the end of the arrow does not change. The maximum of the instantaneous frequency is reached at the same time as the maximum of output pulse intensity, forming a distinct peak in two-dimensional space, which

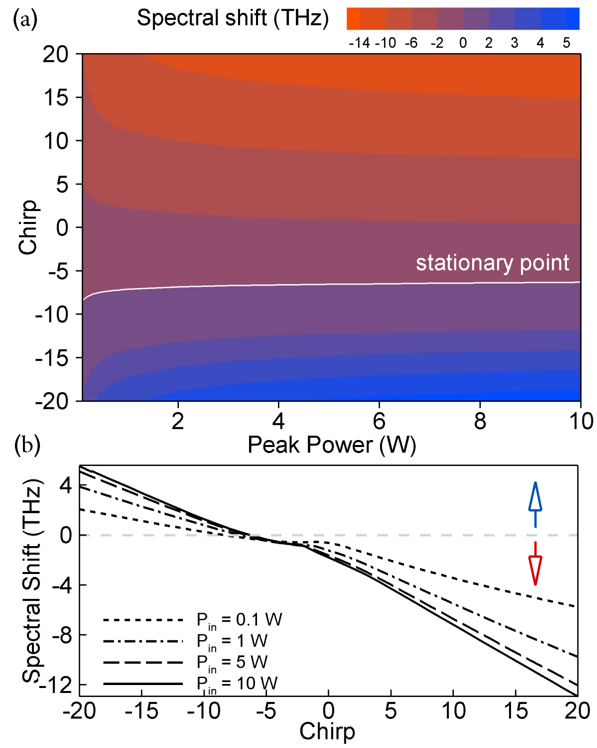

Fig. 1. (a) Spectral shift of the amplified pulse presented in the plane of the peak power and chirp of the initial pulse. Here $T^{in}_{FWHM} = 1$ ps, $G_0 = 30$ dB. (b) Spectral shift of the maximum of the pulse spectrum after SOA for varying input peak power.

y-coordinate corresponds to a spectral shift. Direction and angle of arrows rotation in Fig. 3 is determined by a balance between two terms in the following expression defining the maximum of instantaneous frequency $\Delta\Omega_{max} = max(d\phi_{out}/dt)$:

$$\Delta\Omega_{max} = -C\frac{t_p}{\tau^2} - \frac{\alpha_H(G_0-1)}{2G_0E_{sat}} \times P_{out}(t_p) \tag{4}$$

where $t_p < 0$ is a position of pulse maximum in time. The first term describes the input-pulse chirp while the second term – additive SPM-induced chirp, which does not depend on initial chirp. For small positive chirp $C \sim 5$ two terms are equal (Fig. 3d) and the arrow does not rotate in relation to the initial phase slope. For a zero or negative chirp arrow rotation is counterclockwise (Fig. 3a-c). For a positive chirp rotation becomes clockwise, leading to a well known red shift of the pulse.

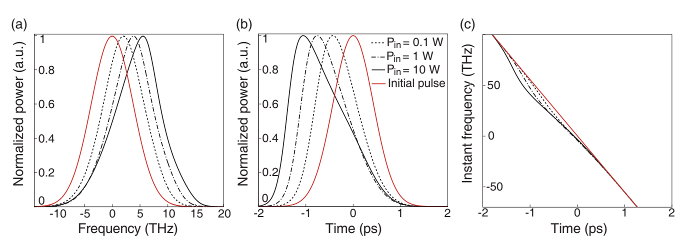

Fig. 2. Pulse spectrum (a), temporal shape (b) and instantaneous frequency (c) at SOA input (red line) and output. $T^{in}_{FWHM} = 1$ ps, $G_0 = 30$ dB, C = -20.

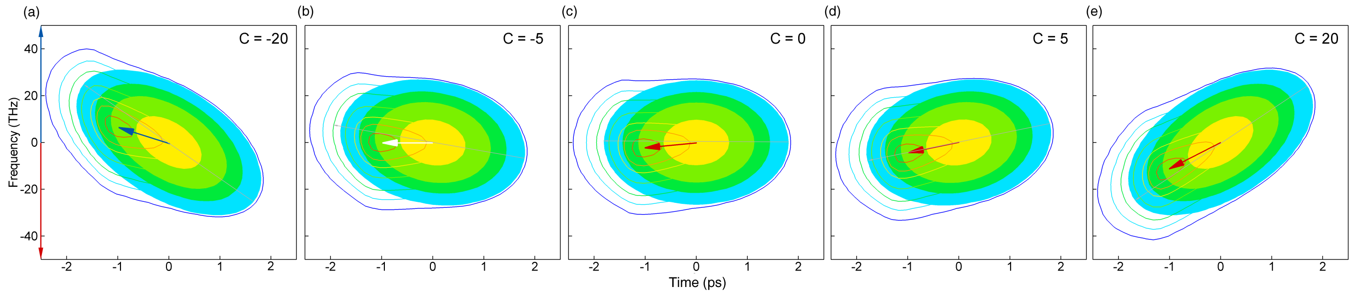

Fig. 3. Pulse spectrogram at SOA intput (filled ovals) and output (colored lines) corresponding to different values of chirp parameter. Blue arrow depicts blue shift of the central wavelength of an optical pulse, red arrows – red shift.

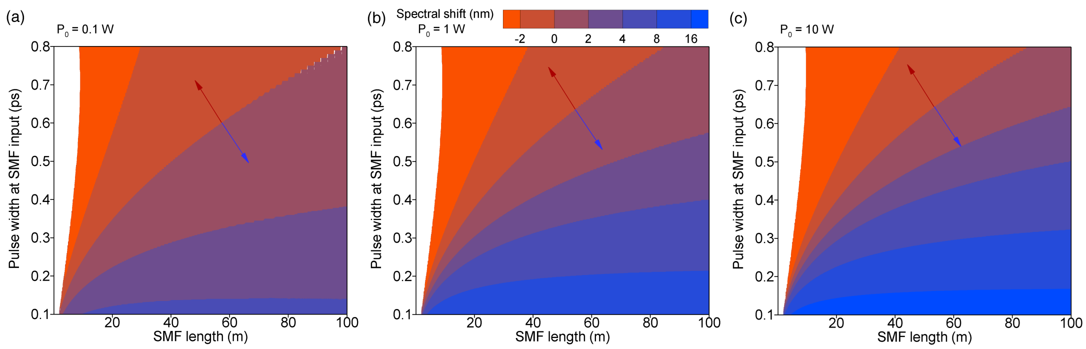

Fig. 4. Spectral shift of the initially unchirped Gaussian pulse with 0.1-10 W peak power after propagation in SMF and subsequent amplification in SOA. Pulse width at SOA input exceeds 1 ps.

Then we examined whether it is possible to realize the blue shift in a simple experimental setup consisting of laser pulse source operating at 1550 nm and single mode fiber (SMF) up to 100 meters long. As a source of ultrashort pulses we have used mode-locked fiber laser based on nonlinear polarization evolution effect. The cavity was comprised of the elements based on SMF-28 fiber, therefore, cavity chromatic dispersion was anomalous. The laser generated nearly Fourier-limited pulses at repetition rate of 14.51 MHz and up to 10 pJ energy. Pulse acquires a negative chirp during propagation in SMF-28 fiber, and passes through SOA (Thorlabs BOA1004P), carrying out the nonlinear pulse transform. Pumping current of the SOA was varied from 0 to 150 mA. At higher values of current we observed significant amplification of broadband background optical noise. Output radiation at SOA output was measured by optical spectrum analyzer Yokogawa AQ6370D with spectral resolution of 0.2 nm. To model pulse propagation in SMF we use generalized nonlinear Shrödinger equation, which takes into account Kerr nonlinearity ($\gamma = 1.1\ \mathrm{W}^{-1}\mathrm{km}^{-1}$), second and third-order dispersion ($\beta_2 = -20\ \mathrm{ps}^2/\mathrm{km}$, $\beta_3 = 0.132\ \mathrm{ps}^3/\mathrm{km}$) and Raman gain. The equation was solved by the standard split-step Fourier-transform method implemented in C++, in which the integration at a nonlinear step was performed using the Runge-Kutta method. The temporal window was equal to 100 ps with 2^{15} points in the grid. The results of simulations are shown in Fig. 4. It should be noted that only the region corresponding to a pulse duration of more than 1 ps at SOA input (after dispersive broadening in SMF) is shown in the figures. Within this region the model of SOA (1) remains valid. Even for a smallest considered peak power $P_0 = 0.1$ W of the initial pulse blue shift is possible if pulse duration lies below 0.8 ps. If we increase peak power at SMF input, blue shift could exceed 20 nm. Figure 5 depicts a comparison of calculated and experimental spectra. Laser pulse with 10 W peak power, 0.8 ps duration and small negative chirp $C = -0.5$ propagates through 20, 40 and 100 meters of SMF and then amplifies in SOA. Both experiment and simulation demonstrate red shift for 20-meters long fiber and blue shift for 40 and 100 meters long fiber. Calculated spectral shapes qualitatively agree with the measured ones.

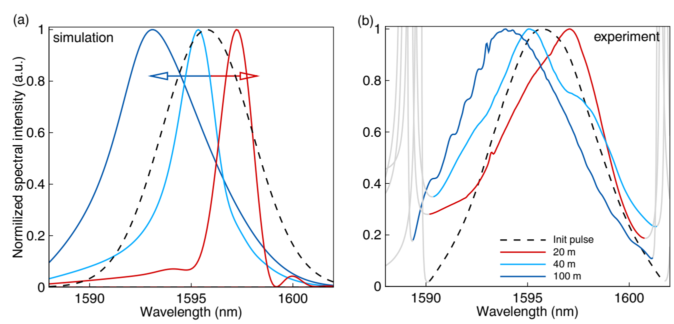

Fig. 5. Normilized pulse spectra after propagation in SMF of 20, 40 and 100 meters long and consequent amplification in SOA in simulation (a) and experiment (b). G_0=27 dB. Experimental spectra features Kelly's sidebands shown by gray lines.

Therefore, even in such a simple scheme the central wavelength of subpicosecond pulses could be shifted to a blue part of the spectrum. Basically, we can use this physical effect to expand the blue part of the spectrum for any spectral interval covered by the semiconductor optical amplifiers in pulsed optical source applications. We would like to point out that the observed effect can find applications beyond simple wavelength converters and optical sources. One of the potential emerging applications where this effect can be usfeul is the development of neuromorphic computing photonic devices. More specifically, our findings potentially might be useful in the design of SOA-based optical neuromorphic devices operating with signal in the spectral domain, either for masking or in the output layer for the reservoir computing systems, see e.g. [18–21].

In conclusion, we demonstrated that optical pulses with appropriate initial chirp can undergo a nonlinear spectral blueshift, opposite to the Raman-induced redshift, when they are amplified by the semiconductor amplifier. The results offer new opportunities for the manipulation and control of the central frequency of optical pulses.

FUNDING

This work was supported by the Russian Science Foundation (Grant No. 21-42-04401).

DISCLOSURES

The authors declare no conflicts of interest.

REFERENCES

1. F. M. Mitschke and L. F. Mollenauer, Opt. Lett. **11**, 659 (1986).
2. J. P. Gordon, Opt. Lett. **11**, 662 (1986).
3. R. Claps, V. Raghunathan, D. Dimitropoulos, and B. Jalali, Opt. Express **11**, 2862 (2003).
4. N. Vermeulen, C. Debaes, and H. Thienpont, Laser & Photonics Rev. **4**, 656 (2010).
5. I. Pupeza, S. Holzberger, T. Eidam, H. Carstens, D. Esser, J. Weitenberg, P. Rußbüldt, J. Rauschenberger, J. Limpert, T. Udem, A. Tünnermann, T. W. Hänsch, A. Apolonski, F. Krausz, A. V. E. Fill volume 7, pages608–612(2013)Cite this articleSokolov, D. R. Walker, D. D. Yavuz, G. Y. Yin, and S. E. Harris, Nat. Photonics **7**, 608 (2013).
6. A. V. Sokolov, D. R. Walker, D. D. Yavuz, G. Y. Yin, and S. E. Harris, Phys. Rev. Lett. **85**, 562 (2000).
7. R. J. Manning, A. D. Ellis, A. J. Poustie, and K. J. Blow, J. Opt. Soc. Am. B **14**, 3204 (1997).
8. T. Durhuus, B. Mikkelsen, C. Joergensen, S. Lykke Danielsen, and K. Stubkjaer, J. Light. Technol. **14**, 942 (1996).
9. M. Matsuura, O. Raz, F. Gomez-Agis, N. Calabretta, and H. J. S. Dorren, Opt. Express **19**, B551 (2011).
10. M. Matsuura, O. Raz, F. Gomez-Agis, N. Calabretta, and H. J. S. Dorren, Opt. Lett. **38**, 238 (2013).
11. V. N. Serkin and V. A. Vysloukh, “Femtosecond spectral tunneling effect in fibers,” in *Conference on Lasers and Electro-Optics,* (Optical Society of America, 1993), p. CFD7.
12. S. P. Stark, A. Podlipensky, and P. S. J. Russell, Phys. Rev. Lett. **106**, 083903 (2011).
13. M. F. Saleh, W. Chang, P. Hölzer, A. Nazarkin, J. C. Travers, N. Y. Joly, P. S. J. Russell, and F. Biancalana, Phys. Rev. Lett. **107**, 203902 (2011).
14. D. Cotter, R. J. Manning, K. J. Blow, A. D. Ellis, A. E. Kelly, D. Nesset, I. D. Phillips, A. J. Poustie, and D. C. Rogers, Science **286**, 1523 (1999).
15. J. Mork and T. W. Berg, Opt. Photon. News **14**, 42 (2003).
16. D. Brunner, B. Penkovsky, B. A. Marquez, M. Jacquot, I. Fischer, and L. Larger, J. Appl. Phys. **124**, 152004 (2018).
17. G. Agrawal and N. Olsson, IEEE J. Quantum Electron. **25**, 2297 (1989).
18. A. N. Tait, J. Chang, B. J. Shastri, M. A. Nahmias, and P. R. Prucnal, Opt. Express **23**, 12758 (2015).
19. L. Butschek, A. Akrout, E. Dimitriadou, M. Haelterman, and S. Massar, “Frequency-multiplexed photonic reservoir computing,” in *Frontiers in Optics + Laser Science APS/DLS,* (Optical Society of America, 2019), p. JW3A.122.
20. T. H. Mitsumasa Nakajima, Kenji Tanaka, Commun. Phys. **4**, 1 (2021).
21. M. Sorokina, J. Physics: Photonics **3**, 014002 (2020).

FULL REFERENCES

1. F. M. Mitschke and L. F. Mollenauer, "Discovery of the soliton self-frequency shift," Opt. Lett. **11**, 659–661 (1986).
2. J. P. Gordon, "Theory of the soliton self-frequency shift," Opt. Lett. **11**, 662–664 (1986).
3. R. Claps, V. Raghunathan, D. Dimitropoulos, and B. Jalali, "Anti-stokes raman conversion in silicon waveguides," Opt. Express **11**, 2862–2872 (2003).
4. N. Vermeulen, C. Debaes, and H. Thienpont, "Coherent anti-stokes raman scattering in raman lasers and raman wavelength converters," Laser & Photonics Rev. **4**, 656–670 (2010).
5. I. Pupeza, S. Holzberger, T. Eidam, H. Carstens, D. Esser, J. Weitenberg, P. Rußbüldt, J. Rauschenberger, J. Limpert, T. Udem, A. Tünnermann, T. W. Hänsch, A. Apolonski, F. Krausz, A. V. E. Fill volume 7, pages608–612(2013)Cite this articleSokolov, D. R. Walker, D. D. Yavuz, G. Y. Yin, and S. E. Harris, "Compact high-repetition-rate source of coherent 100 ev radiation," Nat. Photonics **7**, 608 (2013).
6. A. V. Sokolov, D. R. Walker, D. D. Yavuz, G. Y. Yin, and S. E. Harris, "Raman generation by phased and antiphased molecular states," Phys. Rev. Lett. **85**, 562–565 (2000).
7. R. J. Manning, A. D. Ellis, A. J. Poustie, and K. J. Blow, "Semiconductor laser amplifiers for ultrafast all-optical signal processing," J. Opt. Soc. Am. B **14**, 3204–3216 (1997).
8. T. Durhuus, B. Mikkelsen, C. Joergensen, S. Lykke Danielsen, and K. Stubkjaer, "All-optical wavelength conversion by semiconductor optical amplifiers," J. Light. Technol. **14**, 942–954 (1996).
9. M. Matsuura, O. Raz, F. Gomez-Agis, N. Calabretta, and H. J. S. Dorren, "Ultrahigh-speed and widely tunable wavelength conversion based on cross-gain modulation in a quantum-dot semiconductor optical amplifier," Opt. Express **19**, B551–B559 (2011).
10. M. Matsuura, O. Raz, F. Gomez-Agis, N. Calabretta, and H. J. S. Dorren, "Error-free 320-to-40-gbit/s optical demultiplexing based on blueshift filtering in a quantum-dot semiconductor optical amplifier," Opt. Lett. **38**, 238–240 (2013).
11. V. N. Serkin and V. A. Vysloukh, "Femtosecond spectral tunneling effect in fibers," in *Conference on Lasers and Electro-Optics,* (Optical Society of America, 1993), p. CFD7.
12. S. P. Stark, A. Podlipensky, and P. S. J. Russell, "Soliton blueshift in tapered photonic crystal fibers," Phys. Rev. Lett. **106**, 083903 (2011).
13. M. F. Saleh, W. Chang, P. Hölzer, A. Nazarkin, J. C. Travers, N. Y. Joly, P. S. J. Russell, and F. Biancalana, "Theory of photoionization-induced blueshift of ultrashort solitons in gas-filled hollow-core photonic crystal fibers," Phys. Rev. Lett. **107**, 203902 (2011).
14. D. Cotter, R. J. Manning, K. J. Blow, A. D. Ellis, A. E. Kelly, D. Nesset, I. D. Phillips, A. J. Poustie, and D. C. Rogers, "Nonlinear optics for high-speed digital information processing," Science **286**, 1523–1528 (1999).
15. J. Mork and T. W. Berg, "The dynamics of semiconductor optical amplifiers: Modeling and applications," Opt. Photon. News **14**, 42–48 (2003).
16. D. Brunner, B. Penkovsky, B. A. Marquez, M. Jacquot, I. Fischer, and L. Larger, "Tutorial: Photonic neural networks in delay systems," J. Appl. Phys. **124**, 152004 (2018).
17. G. Agrawal and N. Olsson, "Self-phase modulation and spectral broadening of optical pulses in semiconductor laser amplifiers," IEEE J. Quantum Electron. **25**, 2297–2306 (1989).
18. A. N. Tait, J. Chang, B. J. Shastri, M. A. Nahmias, and P. R. Prucnal, "Demonstration of wdm weighted addition for principal component analysis," Opt. Express **23**, 12758–12765 (2015).
19. L. Butschek, A. Akrout, E. Dimitriadou, M. Haelterman, and S. Massar, "Frequency-multiplexed photonic reservoir computing," in *Frontiers in Optics + Laser Science APS/DLS,* (Optical Society of America, 2019), p. JW3A.122.
20. T. H. Mitsumasa Nakajima, Kenji Tanaka, "Scalable reservoir computing on coherent linear photonic processor," Commun. Phys. **4**, 1–12 (2021).
21. M. Sorokina, "Multi-channel optical neuromorphic processor for frequency-multiplexed signals," J. Physics: Photonics **3**, 014002 (2020).